Research Article

Stephan Bruening*, Arnold Gillner and Keming Du

Multi beam microprocessing for printing and embossing applications with high power ultrashort pulsed lasers

https://doi.org/10.1515/aot-2021-0025
Received May 7, 2021; accepted June 25, 2021;
published online July 20, 2021

Abstract: Micro structuring of surfaces is of great interest for various applications, e.g. for the tooling industry, the printing industry and for consumer goods. In suitable mass production applications, such as injection molding or roll-to-roll processing for various markets, the final product could be equipped with new properties, such as hydrophilic behavior, adjustable gloss level, soft-touch behavior, light management properties etc. To generate functionalities at reasonable cost, embossing dies can be augmented with additional micro/nano-scale structure using laser ablation technologies. Despite the availability of ultrashort pulsed (USP) high power lasers (up to several hundred watts), it is still a challenge to structure large areas, as required on embossing rolls, in an acceptable processing time for industrial production. In terms of industrial implementation, direct digital transfer is a limiting factor for ultrahigh resolution. Shorter machining times by further increasing spot or workpiece motion are limited. Enlarging the ablation diameter, and thus the tool diameter, delivers a higher ablation rate with the comparable ablation quality, but entails a reduction in resolution. While maintaining the achieved state-of-the-art performance, upscaling of single modulated lasers provides a less demanding way to increase productivity. In the processing of steel surfaces, an increase in material removal can also be achieved by using pulse burst. In this work, the parallel process of single modulated multi laser sources is compared with a laser source split by diffractive optical elements (DOE) for applications in a cylinder micro patterning system. A newly developed highly compact ps laser with repetition rates up to 8 MHz and an average power of 300 or 500 W was divided into 8 or 16 parallel beamlets by a DOE. The ablation rate of each approach was investigated by typical microstructures on copper surfaces. At surface speeds of 10 m/s and a resolution of 5080 dpi, an ablation rate of up to 27 mm^3/min was achieved. Different functional surface geometries were realized on an embossing roll as master, which is used for replication of the structures in roll-to-roll processes. Functional structures, such as friction reduction, improved soft touch or light guiding elements on large surfaces are demonstrated.

Keywords: 3D microstructure; acousto optical modulator AOM; diffractive optical element DOE; multi spot; nano imprint lithography (NIL); parallel micro-processing; roll-to-plate roll-to-to-roll micro-embossing; surface functionalization; usp-laser.

1 Introduction – large area microstructuring

Due to an increasing demand for functional requirements for consumer products, such as reduced friction, extended life, improved soft touch or antibacterial effect etc., a targeted adjustment of the surface layer properties is becoming increasingly important for industrial applications. The solution to this requirement is not only to provide the right functionality, but also to adjust the service life of the product. In many cases, the various types of coating technologies do not provide the required lifetime. However, laser processing methods can provide a solution to this problem.

Using laser microstructuring of cylinder surfaces (Figure 1) as a replication tool and replicate the structures on foils in roll-to-roll processes (Figure 2), proper functional surface properties with the required lifetime could be produced. In addition to the function requirements, the production costs, and environmental pollution can also be reduced compared to the costly coating technologies. A

***Corresponding author: Stephan Bruening**, Schepers GmbH & Co. KG, Vreden, Germany, E-mail: s.bruening@schepers-digilas.de. https://orcid.org/0000-0003-0252-1478
Arnold Gillner, Ablation and Joining, Fraunhofer-Institut fur Lasertechnik, Steinbachstr. 15, Aachen, Germany, E-mail: arnold.gillner@ilt.fraunhofer.de
Keming Du, Edgewave, San Diego, USA, E-mail: du@edge-wave.com

typical example of a topography transfer is the natural leather structure, as shown in Figure 3. The resolution is 2540 dpi (pixel size: 10 µm). The grey tone of the pixel describes the depth. For example, black at 100% gives a maximum depth of 200 µm.

For direct structuring of metallic surfaces, engraving times of several days for 1 m^2 would be the result. For rubber-based materials, times would be reduced by 30 min for 1 m^2. In a roll-to-roll process, 4 m^2 of aluminum sheet could be embossed in 1 min. For non-metals, 5 m^2/min could be realized in the nano imprint process [1] or up to 20 m^2/min of plastics could be produced in the hot imprint process and 250 m^2 of paper-based substrates could be imprinted, Figure 5.

Figure 1: Embossing cylinder.

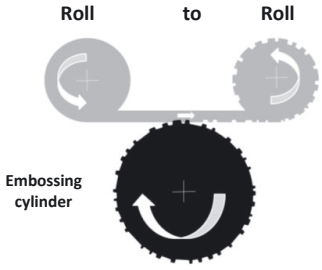

Figure 2: Roll-to-roll process with embossing cylinder.

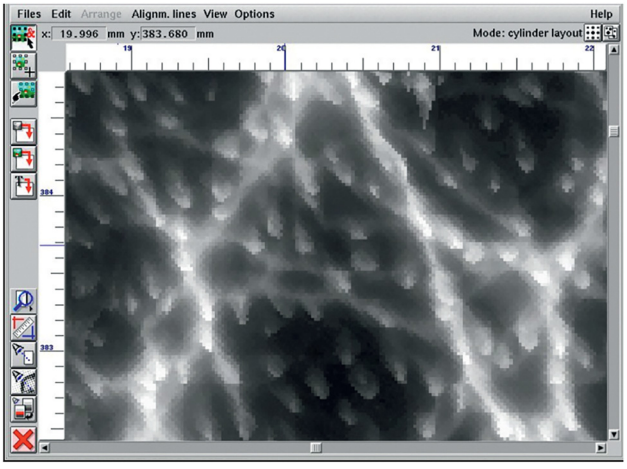

Figure 3: 3D digital data asset natural leather 1270 DPI, magnification: 5×.

Figure 5 shows that for a high productivity, which is necessary for mass production, rotary processes are required. These can be realized with cylinders or rollers as embossing tools, as shown in Figure 1.

Embossing cylinders are the base for a synthetic generation of nano/microstructures as a mass fabrication tool which is used for high precision, large scale, and high-speed micro processes. Microstructuring of the embossing cylinders with ultrashort laser pulses offers many benefits compared to alternative processes, e.g. ns-laser ablation [2]. The ultrashort pulses and the extremely high intensities offer a material-independent ablation with minor melt effects [3]. Latest high-power ultrashort pulsed laser sources ($P_{average}$ = 300 W) boost 3D microstructuring of large-scale metal surfaces for embossing and printing applications with ps-lasers by a significant reduction of the processing time. Although the advantages of ultrashort laser pulses are well known in the industrial micro material processing regarding lateral and depth resolution, there is still a lack of productivity compared to competing procedures especially for applications where large ablation volumes are required.

In previous papers it was shown that a moderate fluence is necessary to achieve very high ablation qualities. A very well-balanced algorithm to generate an ablation process is required, which on the one hand allows smooth processing surfaces and on the other hand, at the same time,

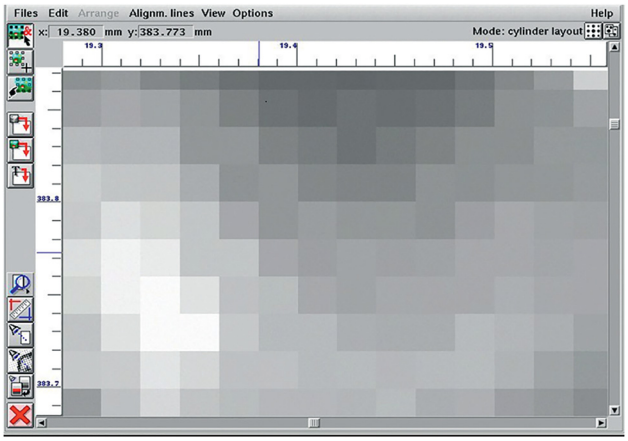

Figure 4: Detail view of Figure 5, magnification: 50×, pixel size: 20 µm.

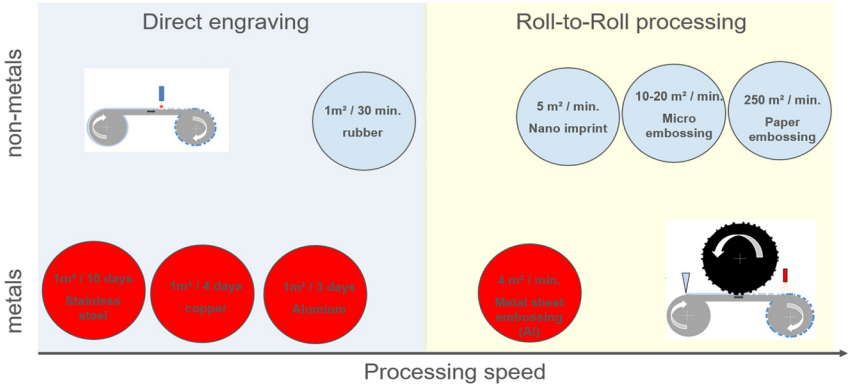

Figure 5: Micro-processing time for 1 m^2 at 200 µm depth and 2540 dpi.

prevents the accumulation of heat and melt residues [2]. With an available pulse repetition rate of ultrafast lasers in the MHz range and the high speed of common cylinder scan devices in the range of 20–30 m/s, the necessary low overlap can be managed [4]. A further increase of the scanning speed presupposes an improvement of several components, such as data processing, modulation velocity, and rotation/beam deflection velocity. A much more convenient and efficient approach to get optimized processing conditions at higher power levels is possible by a multi spot application. To preserve a split in multiple paths, the fluence of each single spot must be kept moderately. A central question in a multi spot application is the interaction between the acting spots and the resulting thermal accumulation on the metal surface.

2 Tooling of embossing cylinders

The outstanding quality of ultrashort pulse lasers with an almost melt-free removal, due to the extremely short pulses, offers fine ablation geometries. With ablation dots down to 2 µm, near the ablation threshold, machining resolutions of 25,400 DPI are possible. For achieving acceptable processing times with these fine resolutions, a high-speed scanning application, as offered by cylinder micromachining systems, is required to provide the necessary efficiency. In combination with high repetitive lasers, it is possible to enable this high-speed scanning application with pulse to pulse overlaps of 50%. For example, to realize a 50% pulse overlap with a spot size of 2 µm at 10 m/s, a pulse repetition rate of 10 MHz is necessary.

2.1 Data handling

Generating 3D structures with depths of several 100 µm in one operation (one layer) is not possible as due to the low thermal penetration depth of USP laser, the resulting material removal depth per layer is up to 1 µm (several 100 nm per pulse), even with multiple pulse overlapping from spot to spot. A depth of several 10 µm, which is necessary for embossing elements like leather structure (Figure 3), can therefore only be achieved by multiple engraving layers. Generally, the process corresponds to an image setter principle, i.e. the laser will be controlled, pixel by pixel, through a bitmap data asset (Figure 4). The depth information of the leather structure is defined through the halftone value of each pixel, as shown in Figure 6 Left. The 8-bit halftone image will be subdivided into 1-bit files, which, in turn, represent the individual layers to be removed (Figure 6 Right). Thus an 8-bit dataset is made up of a maximum of 255 1-bit datasets depending on the desired structure depth.

In consideration of the 1 m by 1 m area, a file with a resolution of 5 µm per pixel will exceed the 4 GB limit in Windows based systems, even with a 1 bit file. To get around this limit, the DIGILAS uses big TIF data assets. In addition, the step size of the layers is defined by the material removal per layer which, in turn, determines the depth resolution. The engraving data is prepared in such a way that a halftone value is assigned to a certain depth and thus a defined number of layers, as described in Figure 7. The material removal per layer is inversely proportional to the possible depth resolution and is dependent on the metal to be structured. During the engraving process, the control software tracks the focal position from layer to layer. Particularly with deeper structuring (several 10 µm), the focal position must be tracked in order to keep it within the range of the focal depth, and thus to guarantee constant material removal conditions. The typical layer based micro-processing method was enhanced to a machining technology in which several layers could be processed within one path. According to an 8-bit data set, one modulator per channel individually controls the fluence of each spot from pixel to pixel.

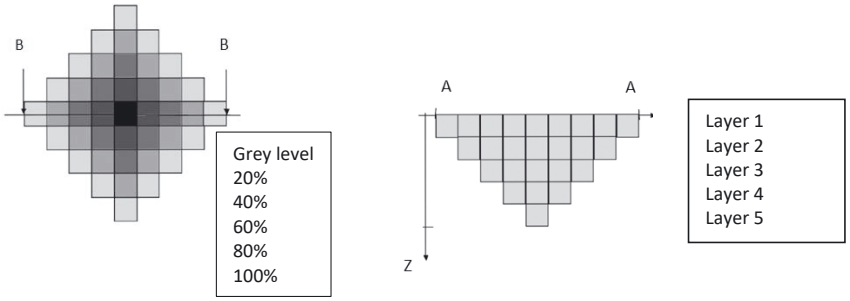

Figure 6: **Left**: 8-bit data asset with five grey levels. **Right:** Cross section/five grey levels to five layers.

2.2 Ultrahigh precision cylinder micro-processing system

To avoid negative heat accumulation and resulting excessive ablation of the surface, the individual pulses must be separated during the removal. Otherwise the ablation behavior will be changed, and the surface quality will be significantly decreased because of melt residues [5, 6]. In hole drilling applications this effect cannot be solved because the pulses are always placed at the same position. To achieve a minimal thermal process, the pulse repetition frequency must be adjusted. For a surface removal method in which the workpiece is scanned in a meandering way, the pulses can be placed side by side. In this case, the required pulse repetition frequency is determined by the scan speed. Oscillating mirror systems or galvanometer scanners can be currently driven with speeds of up to 5 m/s. With a spot diameter for example of 24 µm a maximum pulse sequence frequency of 125 kHz can be applied in order to avoid pulse-to-pulse-interaction. In this case the process speed is limited by the scanner, as lasers with ps-pulse repetition rates of 4 or 8 MHz are already commercially available [3, 5, 7].

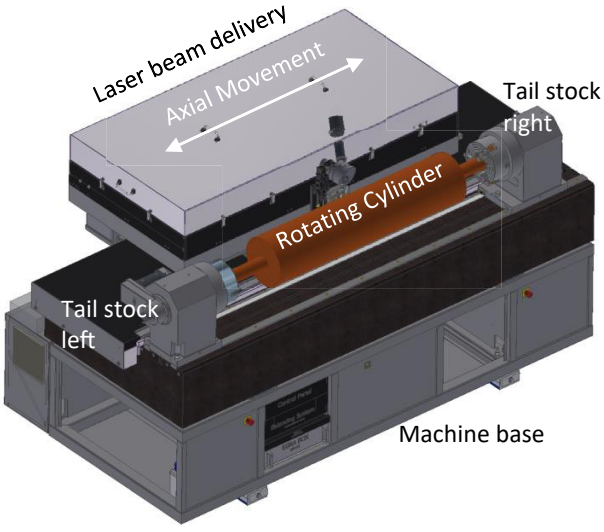

Figure 7: Schematic of a cylinder processing system.

A machining system with a high systematically scanning speed is a cylinder scanning system (Figure 7), which is generally used for engraving of embossing and printing cylinders. As the workpiece (Figure 2) is rotationally symmetrical, a very high uniform peripheral speed can be achieved [3, 8]. It is advantageous that the synchronization process between moving workpiece and laser source since no acceleration conditions and delays are applied in comparison to galvanometer scanners. Thus, in this application, scanning speeds of up to 50 m/s are possible. For example, at a surface speed of <50 m/s and a pulse repetition frequency of 10 MHz, a minimum pulse overlap of 60% is possible. By even higher pulse repetition frequencies, the system moves more and more in a cw mode. For generating a high productivity with a constant ablation quality at a high pulse repetition rate, the pulse interval must have an adjustable overlap of 0–90%. Beside the control of the high velocity, the position stability of the rotating axis is in the sub µm range. The positioning of the laser head in a cylinder processing system is in the range of +/−200 nm for an engraving width of 5 m.

2.3 High power ps-laser source

For scaling up power and energy of a laser system, generally oscillator and amplifier systems (MOPA) like INNOSLAB systems are used [5]. The new high power slab laser contains a Nd:YVO4 mode locked oscillator generating 50 MHz, 10 ps pulse train, and an average power of 1.7 W, a pulse picker and an amplifier. The beam quality factor is $M^2 = 1.3$. Figure 8 shows the schematic of the slab amplifier system. The slab amplifier is split in two stages. A multi-pass slab amplifier for the first stage and a single pass amplifier for the second stage was adopted.

The output power of the first stage is 100 W and that of the second stage amplifier is designed for an average power of 500 W @ 1064 nm. Figure 9 shows the intensity distributions in the near-field and in the far-field. The near field was obtained by using the intensity profile at the laser exit

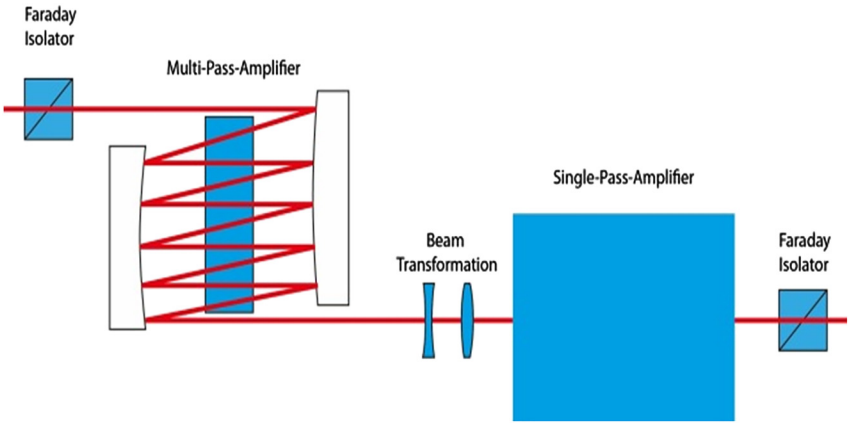

Figure 8: Schematic of the slab–amplifier system.

window. The far filed was obtained by measuring the intensity distribution in focus of a 500 mm positive lens. They are Gaussian, which was applied for all investigations in this paper. The beam quality is $M^2 < 1.2$ in both directions.

After the amplification an electrical optical modulator attenuates the output power level, as shown in Figure 10. The optical modulator consists of a Pockel cell and a thin film polarizer. The Pockel cell is driven by a high voltage module. By changing the voltage from 0 to a half-wave voltage the output power can be adjusted from zero to 100%.

3 Increasing the ablation efficiency

3.1 Single spot application with adapted spot size

As described before, cylinder laser engraving systems allow pulse-to-pulse spacing with highly repetitive ultrashort pulse lasers in the multi MHz range, solely by fast moving workpieces, without the need for an additional fast scanning system for spot movement. Only the dynamic system "rotating cylinder" is responsible for the precision of the positioning of the laser spot, as all other components behave statically in comparison. This allows that the spot-to-spot distance is adjusted even with large spot diameters. In this way, high average laser powers, with the ablation properties typical for ultrashort pulse lasers, can be realized. However, the disadvantage is that the possible lateral resolution also decreases with an increasing spot diameter. If a resolution of 2540 dpi or higher is desired, only the following two methods are suitable.

3.2 Combining multi laser sources

In microstructuring applications, where the lateral resolution is secondary and where the advantages of a melt-free removal are desired, spot diameters of approx. 50 µm can be used in some cases. For producing the necessary fluence with these relatively large ablation diameters, the entire

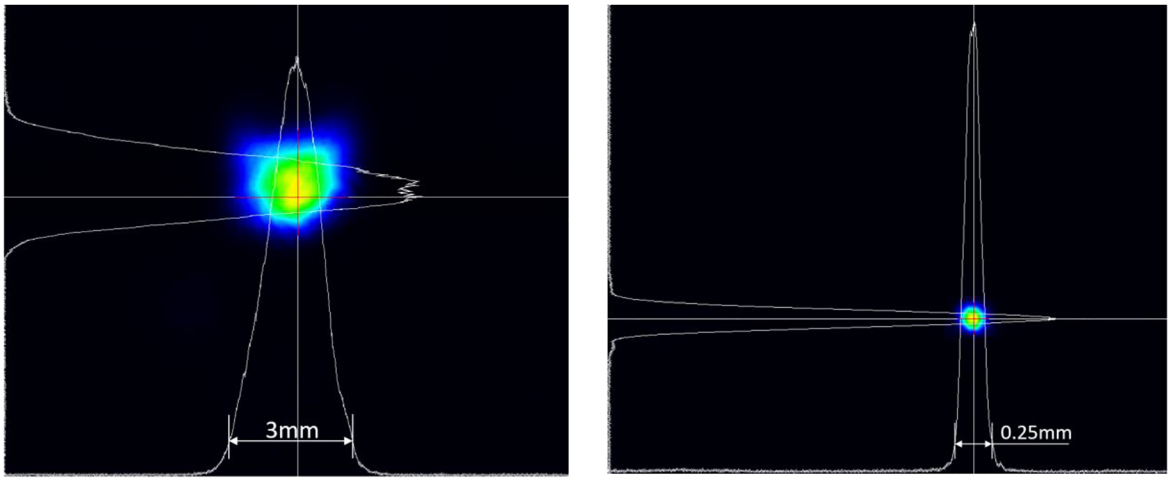

Figure 9: Beam profile 500 W laser in near-field (left) and in far-field (right). The beam quality is $M^2_x = 1.16$, $M^2_y = 1.06$.

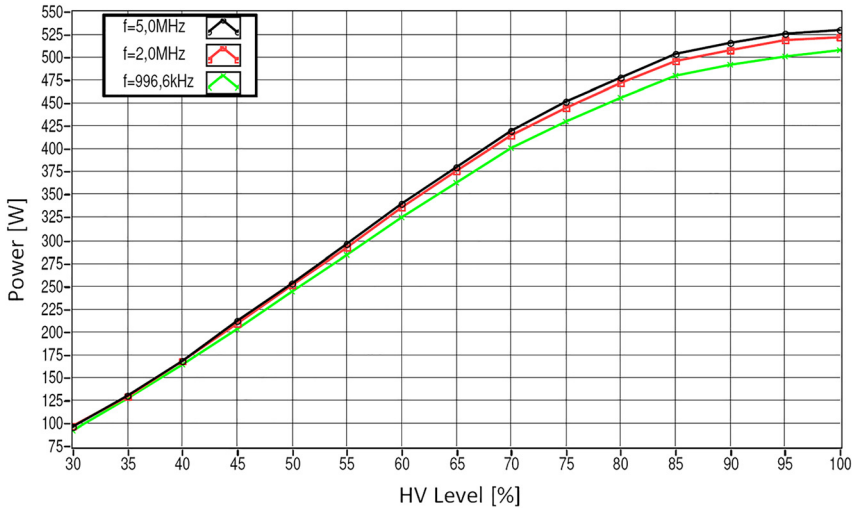

Figure 10: Laser output power vs. HV-level of electro optical modulator, pulse repetition rate 1 MHz (green), 2 MHz (red), 5 MHz (black).

pulse energy of a single beam source must be used. A possibility to reduce the processing time in these cases is the scaling up of laser sources. If high power ps-laser radiation could not be transferred by fibers, a compact setup is a challenge. A beam delivery with one focusing lens allows a compact system set-up. The requirement for high compactness limits the maximum number of combinable lasers. In Figure 10, the merging of four laser beams is schematically shown. Due to this arrangement, the spots can be placed at a distance of some 10 µm in the focal level on the substrate which allows a very compact machining head. Through a defined beam propagation angle to each other, a telecentric set-up could be realized. The pulse frequencies of the individual lasers could be synchronized to each other in order to not influence the plasma created by the single pulses.

3.3 Splitting one laser beam in several spots

If smaller spot sizes are obtained and the pulse energy of one laser can serve multi laser spots (>8), the division of a laser beam out of one single beam source will be most efficient (Figure 11). The approach used for the investigation shown in chapter F is based on a diffractive optical element which splits the beam in a defined number of spots. The beam size and divergence angle must be adjusted before the laser source is split into several beam orders. The beam orders will spread in defined angles before a Fourier lens collimates all beams to generate the correct beam propagation into a multichannel acousto-optical modulator. In our approach, the beam comb after the modulator will be spatially compressed by a pair of prisms to allow a beam delivery with smaller optics. The ablation area is formed by a set-up of two lenses [4].

The principle of applying multi laser spots by splitting one laser in several beam paths or combining several lasers to a multi spot system is defined by the desired resolution, and respectively by the size of the ablating spot.

4 Single spot in a fast cylinder micro-processing system

For the experiments a newly developed ps-laser (pulse duration 12 ps) with repetition rates of up to 8 MHz and an average power of 300 W was investigated. By means of a fast-rotating workpiece (cylinder) for pulse separation, the maximum usable laser power and thereby the maximum ablation rate was investigated at an adapted ablation diameter of up to 50 µm to achieve moderate fluence. The experimental ablation rates were evaluated by engraving 150 µm^2 cells, as shown in Figure 12.

These cells were ablated with different fluence (2.5, 3.4, 4.6, 4.9, and 5.1 J/cm^2, adjusted by an external pulse picker) and machined with a scanning speed of 25 m/s with a machining resolution of 2540 dpi. The results of this

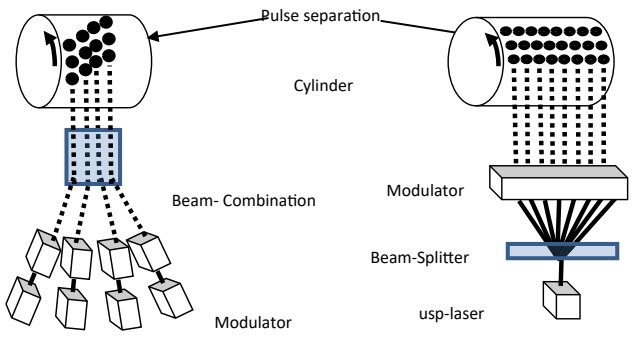

Figure 11: Splitting of one laser source.

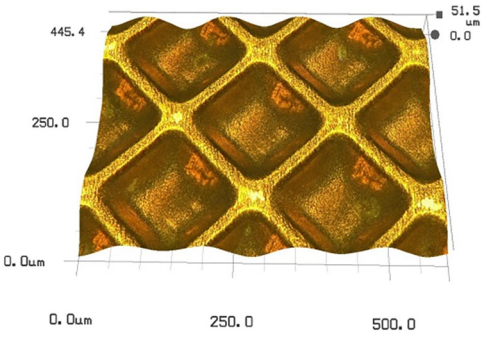

Figure 12: Gravure cell, copper, size 150 µm², depth: 50 µm.

investigation are shown in Figure 13. Three different materials, steel X1.4310, copper, and brass were investigated.

The maximum ablation rate of 42 mm³/min was achieved with the material brass. The ablation rate in copper was nearly 25 mm³/min and in steel 17 mm³/min. Besides the ablation rate, the contour accuracy between the digital image data and the produced geometries are of major interest when comparing the characteristics of the picosecond approach with the nanosecond processes. Contour and geometry accuracy are also influenced by larger spot diameters, even if the pixel accuracy of the machine is in the range of 10 µm. Therefore, an optimum must be found between machine resolution and achievable ablation rate. Generally, the ablation behavior with respect to ablation depth per pulse, surface roughness, residue, and burr is similar to smaller spot sizes with a low power laser ($P_{average}$ < 100 W) and comparable fluence. Independent to the resolution or structure size with 300 W average power, the contour accuracy could be achieved, as shown in Figure 13.

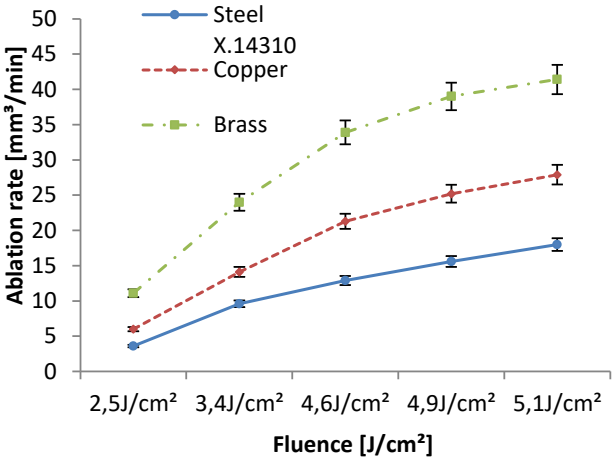

Figure 13: Ablation rate, ablation diameter: 50 µm, 300 W ps-laser.

Depending on the microstructure size to be achieved, an adequate spot size must be adjusted. In consideration of a machining fluence of approx. 5 J/cm², the average power must be decreased for higher resolutions. With a smaller spot size and a lower average power, the ablation rate is decreasing in the same manner (Figure 14).

By means of the investigated 300 W ps-laser and a preset pulse energy of 150 µJ at 2 MHz, the maximum ablation rate of 27 mm³/min with a fluence of 5.1 J/cm² in copper was achieved. For a further reduction of the processing time, a coupling of several laser sources is inevitable to realize a multi spot application, as described in Section 3.2 combining multi laser sources. For example, with a combination of four laser sources with an overall average power of 1200 W an ablation rate of 108 mm³/min in copper is expected. If higher resolutions are obtained, the spot size and accordingly the pulse energy will decrease. This means that the laser power must be reduced. Nevertheless, to transfer the laser power into a maximized ablation rate, the laser must be split into multi spots.

5 Multi laser application/pulse burst mode

For an efficient process set-up of a multi spot array/row, the spot distances must be very close, as each spot must track along the entire surface. A telecentric set-up allows distances of the spots in the range of some 10 µm. Larger spot distances would lead to higher processing times and reduce the advantage of the multi spot application (Figure 15).

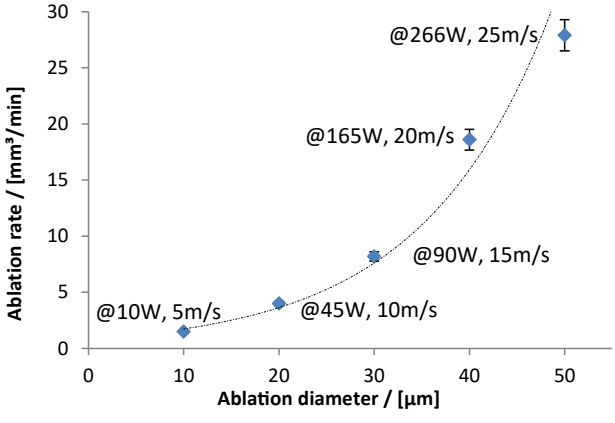

Figure 14: Laser power and corresponding ablation diameter vs. ablation rate of Cu (dashed line is a fit to highlight the increase), wavelength: 1064 nm, pulse duration: 10 ps, pulse repetition rate 2 MHz.

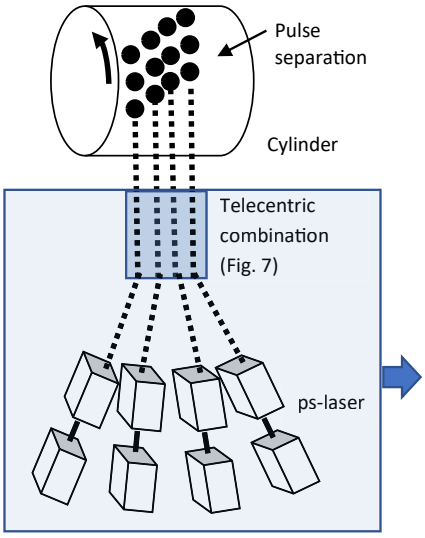

Figure 15: Multi laser application.

A close placement or the complete overlap of the circumferential laser spot lines will lead to an increased pulse-to-pulse interaction. To avoid or to minimize this interaction, the laser sources are synchronized to each other. Besides the synchronization of the pulse repetition, described in the previous chapter, the spatial synchronization of the spots in an accuracy of +/−100 nm on the surface must be realized. The synchronization of the lasers is based on scales and given by a software algorithm which allows a defined placement of the spots in axial and circumferential direction. The laser is the master and defines the zero position in both axes. Based on this orientation, the other lasers will be synchronized by the delays/offsets *x*1, *x*2, *x*3 in axial direction and *y*1, *y*2, *y*3 in circumferential direction (Figure 16). The accuracy of the scales is in the range of 50–100 nm [9].

The described approach of scaling laser sources is a solution for an increased throughput in a cylinder processing system. The combination of parallel lasers in one beam delivery set-up scales up the ablation rate with the number

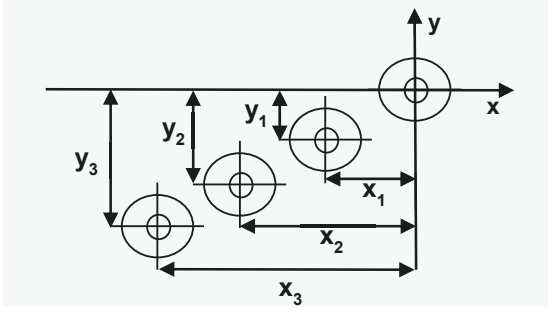

Figure 16: Spatial synchronization of multiple lasers..

of spots. The ablation rate of e.g. steel X1.4310 at 1 MHz with a fluence of 8.9 J/cm^2 and a pulse burst of 8 enables an ablation rate of 3.65 mm^3/min. Four parallel acting laser spots increase the ablation rate up to 14.6 mm^3/min (Figure 18) and keep the quality level of the single spot application. Due to the well-balanced combination of machining parameters and pulse burst mode, structure depths of several 100 µm are possible with a constant surface roughness without any artefacts.

However, the results show a rather large impact on the spot distances considering the achieved quality and ablation rate. In the test set-up, a space of minimum 80 µm between the ablation zones was necessary to provide the constant quality level as achieved with the single laser application. The quality aspects of two-dimensional rotogravure cells (Figure 19) were investigated.

Besides steel X1.4310, the materials brass and copper were investigated in the set-up. Compared to previous investigations [2], the ablation rate of these materials could

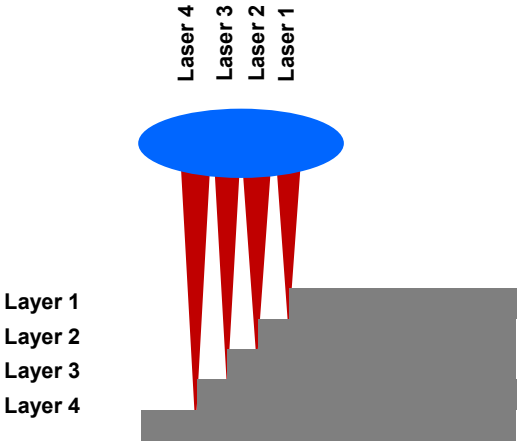

Figure 17: Assignment of laser to layer..

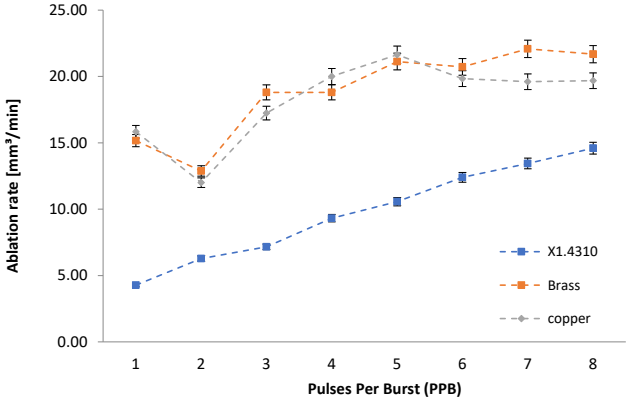

Figure 18: Ablation rate of X1.4310, brass, copper, processing parameter: Tab. 1, four laser spots: 4× 8.9 J/cm^2 vs. pulses per burst.

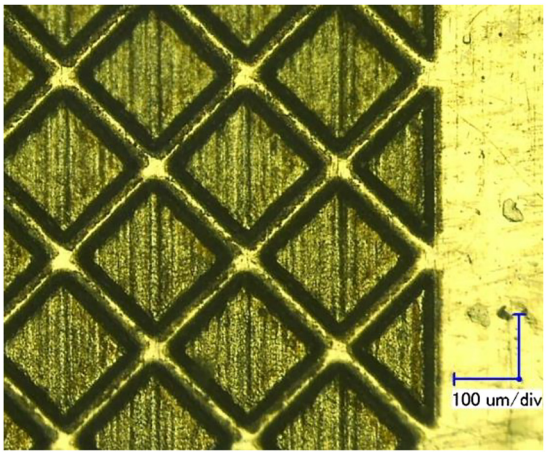

Figure 19: Rotogravure cells on X1.4310 surface, cell width 140 µm..

be increased with the number of laser spots. With four spots and an overall average power of 176 W (rep.-rate: 1 MHz) brass and copper show a maximum ablation rate of 22 mm³/min. The ablation behavior of brass and copper depends on the applied number of pulses in a burst and differs significantly from that of the steel substrate. Steel X1.4310 shows a continuous rise of the removal rate dependent on the applied number of pulses within a burst. Results without cone like protrusions (CLP's) were achieved at pulses in a burst higher than three. Obviously, the ablation rate of copper and brass could be increased with the number of pulses, but a continuous rise of the ablation rate could not be recognized, as it was the case with the steel substrate. Therefore, in case of brass and copper the number of pulses in a burst should not exceed the number of three. At higher number of pulses in a burst, melt and residues occur. The evaluated parameters have been transferred to a 3D layer processing of X1.4310. Based on an ablation of one µm determined in the previous investigations and the total engraving depth to be achieved, an 8-bit greyscale image was divided into layers. Each layer is again a separate greyscale image. This engraving stack was then transferred to the surface layer by layer. In Figure 20, the different ablation layers can be recognized by the height lines in the relief of the processed micro "Schiller" head.

6 Multi spot system by splitting a high power usp laser

For a high precision micromachining, fluence near the ablation threshold provides the highest depth resolution. In consideration of the small spot size and the resulting low pulse energies, one laser source is sufficient to serve several spots and enable the maximum ablation of a high-power ultrashort pulsed laser source. In combination with a high scanning speed with simultaneous high repetition rates (up to 3 MHz), a multichannel acousto-optic modulator (AOM) offers some advantages. In a cylinder processing system with surface speeds up to 50 m/s, the multi beam modulation has only the task to distribute the laser power into several channels in order to minimize the thermal in fluence. The combination of a multi spot array and a fast axis (cylinder rotation) is highly efficient. For the beam splitting a smooth diffractive surface DOE based on fused silica was used [3], providing a 9- and alternatively a 17-channel separated beam splitter design. One of the diffraction orders was out-coupled and used for power reference leading to an eight and 16-channel beam delivery. The fine pulse energy adjustment of each beam could be achieved by modification of the acoustic field of the modulator, changing the diffraction efficiency of the Bragg grating of the acousto optical device. Due to the principle, an adaption to different wavelengths is possible, so that it can be transmitted from 1064 to 532 nm and 355 nm.

6.1 300 W ps-laser/8 beamlets

In a first step the 300 W ultra short pulsed laser was investigated with an 8-spot set-up. The splitting of a single high-power laser beam into a defined number of spots by a diffractive optical element (DOE) offers a compact system [10].

The general concept is shown in Figure 21 and described in detail in ref. [9, 11]. A laser beam SRC with

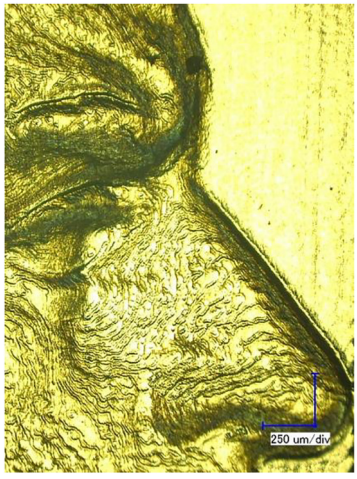

Figure 20: Ablation of a 3D geometry in steel X1.4310, depth: 100 µm..

300 W (1064 nm and 10 ps pulses), optimizes regarding size and divergence angle, is split by a diffractive optical element (DOE) BS into 9 beam orders with defined propagation angles. A Fourier lens focuses FL1 and parallelizes FL2 the beams for the correct coupling into an 8-channel acousto-optical modulator BD-AOM. The beam comb after the modulator will be spatially compressed by a pair of prisms to allow a beam delivery with smaller optics (pAC-cx and pAC-cv). The multi spot intensity distribution at the ablation area is formed by a set-up of three lenses TL1, TL2, TL3 and can be rotated around the propagation axis by a Dove prism DP [2].

The important factors of this multi beam set-up are the pitch precision, the spot uniformity and the efficiency of the beam splitting by the DOE in combination with the AOM. The pitch in the target plane is 20 ± 0.5 µm and the $1/e^2$-spot diameter is about 8 µm. The non uniformity among the maxima is below 16% (Figure 22), and the overall efficiency is about 78% in the target plane.

Each spot in the beam comb can be modulated separately by the acousto-optical modulator AOM according to the grey levels of the engraving data, which allows for equalizing of the non uniformity.

The vertical lines (created by laser pulses) in Figure 23 were engraved in copper surface at a pulse repetition rate of 1 MHz and a surface speed of 15 m/s. The spots show an ablation diameter of about 14 µm with a horizontal distance of 23 µm and could be observed within a focal depth of +−40 µm, as shown in Figure 5.

The experimental ablation rates have been evaluated by engraving areas of rotogravure cells (Figure 24) of 100 × 100 µm.

After synchronization of the eight beams the set-up was tested with 300 W laser power, 3 MHz pulse repetition rate and different fluence (1.6, 3.2, 4.8, 6.4 and 7.9 J/cm^2, adjusted by an external pulse picker) by engraving rotogravure cells with a diagonal size of 83 µm and a wall width of 35 µm at a resolution of 2000 l/cm in circumferential direction (with a surface speed of 16 m/s) and 5000 l/cm in

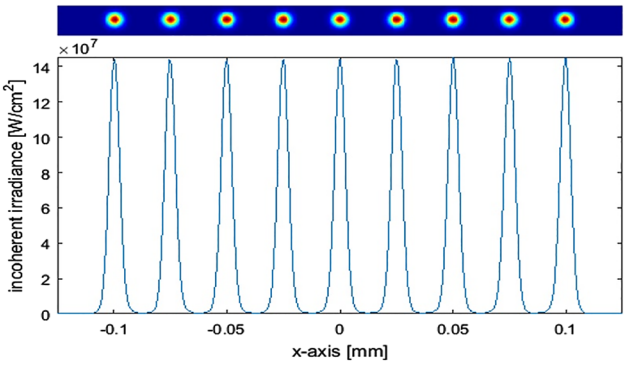

Figure 22: Beamlets in target plane.

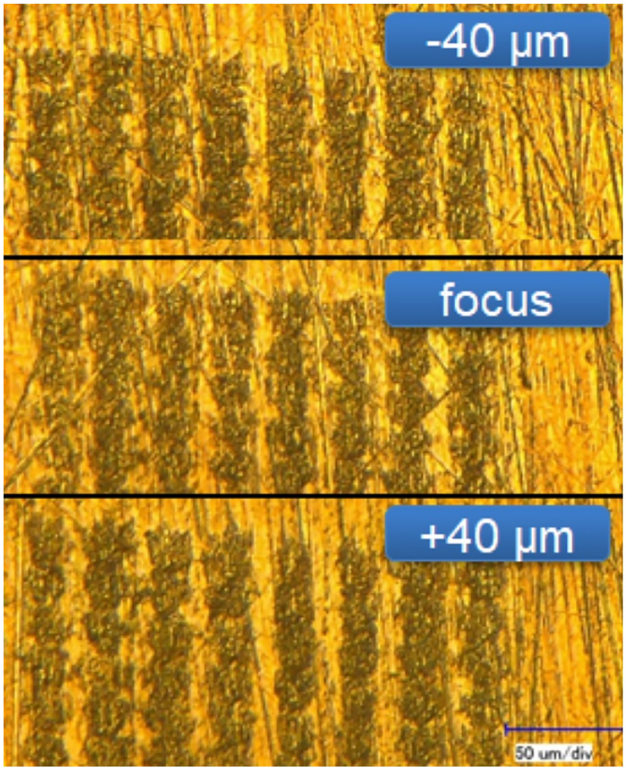

Figure 23: Ablation of eight parallel spots, horizontal, vertical distance given by surface speed of 15 m/s.

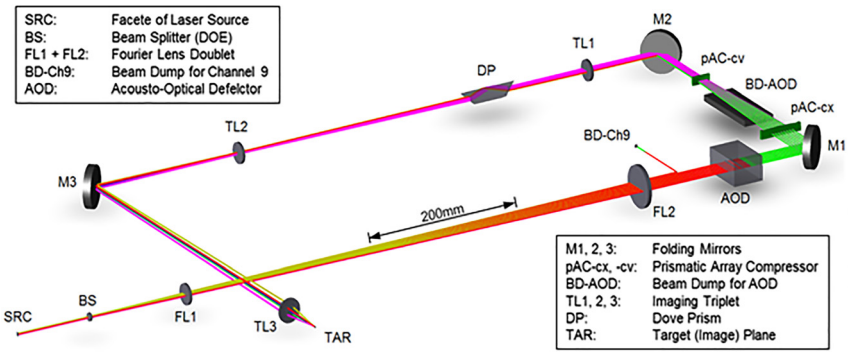

Figure 21: Diffractive beam splitting of a 300 W laser into eight independently modulated beams, each about 29 ± 1 W at focus..

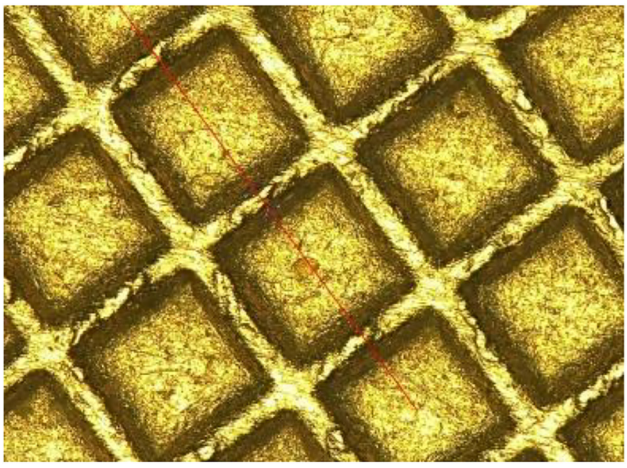

Figure 24: Ablated rotogravure cell, depth: 24 µm, diagonal size 100 µm × 100 µm.

axial direction. The achieved ablation depth/layer was 4 µm, respectively, 24 µm after six passes [8]. This equates to an ablation rate of 16.3 mm^3/min in copper (approx. 2 mm^3/min per beam) (Figure 25).

Based on the evaluated machining parameters, 3D data assets have been transferred by a layer-based processing in a copper surface. A variety of 3D structures on a die for hot stamping applications have been realized and shown in chapter G.

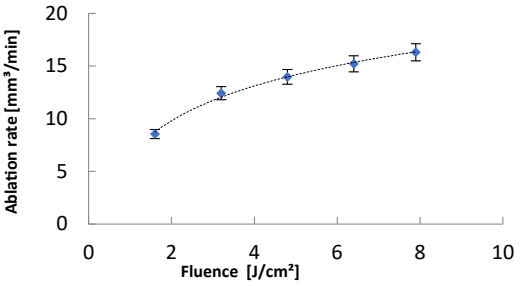

Figure 25: Ablation rate of 8 parallel spots, depending on the fluence, in copper.

6.2 500 W ps-laser/16 beamlets

In a further step an acousto-optical modulator laser with an average power of up to 500 W has been used to increase the number of beamlets. Assuming that the adequate fluence for engraving copper dies is approx. 4–5 J/cm^2, it can be estimated that the developed 500 W slab-based ultra short pulsed laser driven at 1 MHz could be implemented into a processing head that generates 16 beamlets with similar efficiency and the same spot size. A 1-to-17 smooth diffractive beam splitter in combination with two eight-channel AOMs arranged along the optical path concept reduces the pitch to 2 mm (Figure 26) [8].

Analog to the eight-spot system, the multi spot intensity distribution at the ablation area is formed by a set-up of three lenses TL1, TL2, TL3 and can be modulated through the acousto-optical modulators. Due to the spatially restricted acoustic field per beamlet, the interim range of the acousto-optical modulator crystal could be used for transferring every second beamlet without significant influence. A sophisticated arrangement of two 8-channel acousto-optical modulators, as it is shown in Figure 27, provides a sequential switching of the beamlets, according to the propagation direction.

Owing to the longitudinally separated switching planes in combination with only one mirror, providing the Bragg angle of the AOM, an acceptable small lateral shift of <30 µm of the beamlets, perpendicular to the beamlet comb axis, is achieved, as shown in Figure 28. This misalignment of the position can be compensated by a software synchronization adjustment. Thus, the associated prism array pairs for beamlet comb compression can also be neglected.

In Figure 29 the distances of the 16 spots from Figure 28 could be practically approved by engraving all beams parallel a data asset of a triangle structure. The pictures show two rows (distance 40 µm) of each 8 triangles. The distance of the triangles in each row is 80 µm. Figure 30 shows the engraving after synchronization of all acting spots.

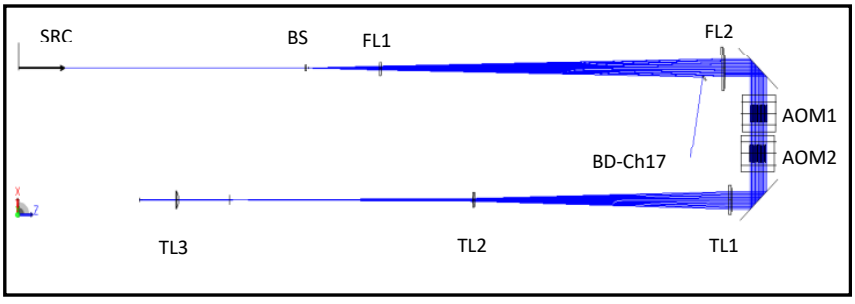

Figure 26: Schematically beam propagation of the 16-spot beam delivery analogue to Figure 21.

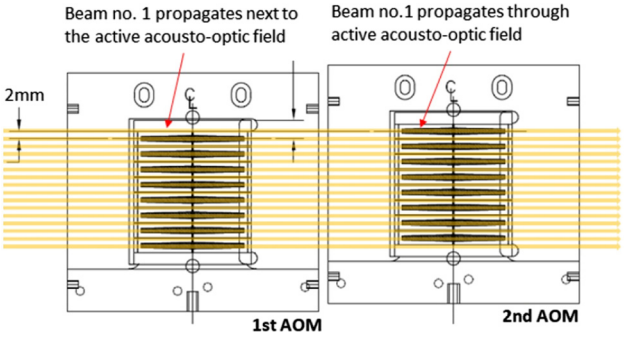

Figure 27: Arrangement of two 8-channel AOM's with a 2 mm orthogonal shift as shown in Figure 26 AOM1 and AOM2.

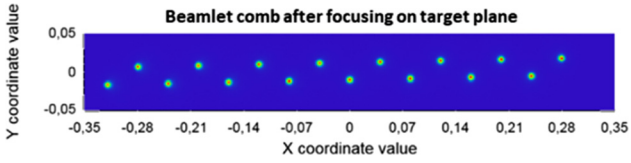

Figure 28: Theoretically determined spot positions in the focal plane caused by AOM1 and AOM2.

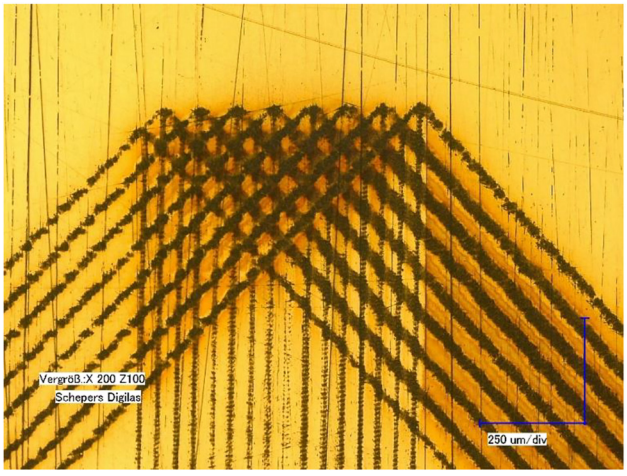

Figure 29: Ablation of 16 parallel acting spots without synchronization in Cu.

After synchronization of the 16 beams the set-up was tested with 500 W laser power and at 1 MHz repetition rate and different fluence (2.2, 4.1, 7.9, 10.9, and 13.2 J/cm^2, adjusted by an external pulse picker) by the rotogravure cell from Figure 6 with a surface speed of 15 m/s. The achieved ablation depth/layer was 8.5 µm, respectively 85 µm after 10 passes. This equates to an ablation rate of 27.09 mm^3/min in copper (approx. 1.7 mm^3/min per beam) (Figure 31).

But since each beam path must be modulated externally by a separate modulator per spot, the maximum

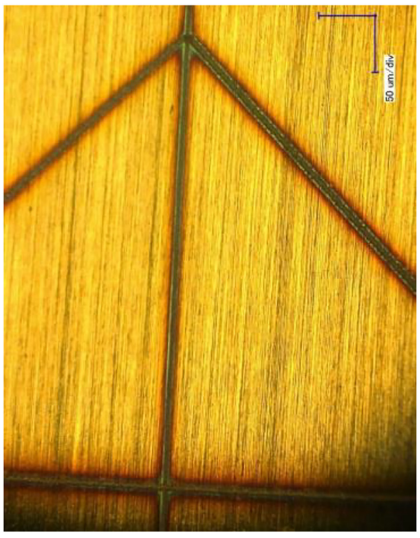

Figure 30: Ablation after synchronization of all acting spots.

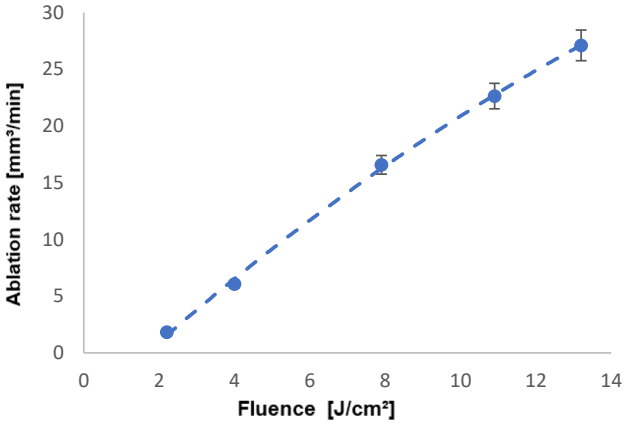

Figure 31: Ablation rate of 16 parallel spots.

number of this multi spot approach can serve between 16 and 24 spots. The reason for a limitation in this case is not the laser power, since ultrashort pulsed lasers are available in the several 100 W region. Using a 500 W laser and single spot energies of less than 10 µJ, more than 50 single beams could be realized. The limiting factors are the size of the modulator-crystal, the beam delivery optics and the focusing optics. Hence, the concept of laser beam splitting is limited, a further scaling up of the multi spot arrays could overcome the limit.

With the use of a multi spot approach thermal issues in the ablation region must be considered. However, if the distances of the single spots are larger than the spot size, as it is the case in the current set-up, and the distance of the subsequent pulses is large enough, in our case the distance of subsequent pulses is 15 µm and there is no overlap of subsequent pulses, thermal accumulation does not occur.

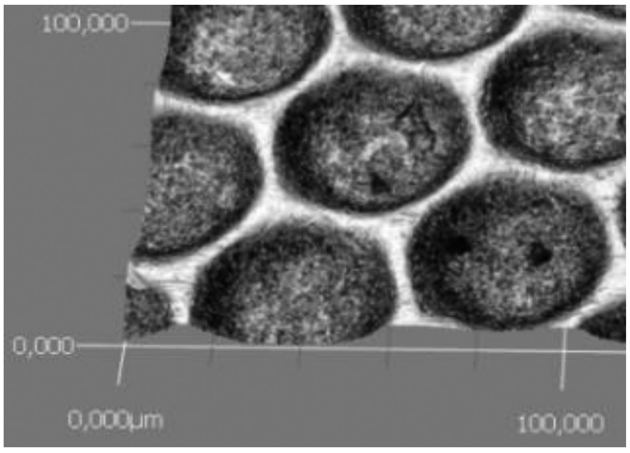

Figure 32: Soft touch structure: diameter: 45 µm, depth: 10 µm.

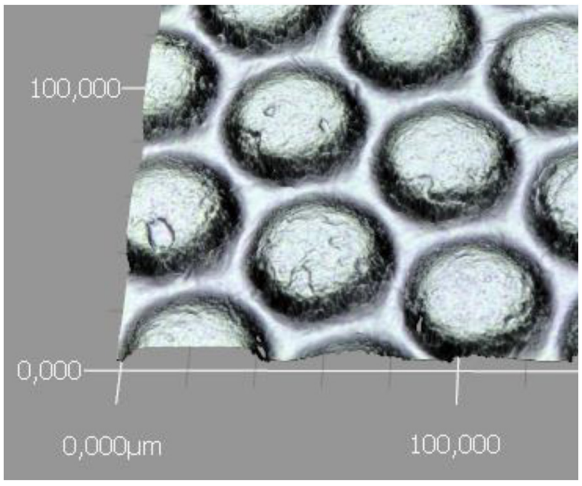

Figure 33: Replica from die, shown in Figure 32.

7 Examples for surface functionalization

Specific surface functionalities can be generated through topographic modifications of the surface. For bio medical, soft touch and optical applications, the dimensions are in the nm up to µm range combined with a low surface roughness and high aspect ratios. The design of those topographies is mostly based on parameter criteria which are known for influencing the interface functions. For optical applications, several software tools are available to create functionalized pixel-based data, which could be used for laser processes. The following examples were processed with a 1064 nm respectively 532 nm, 10 ps pulse duration, and 2 MHz pulse repetition rate.

7.1 Micro structures to reduce skin friction

Skin rubbing on plastic surfaces can be adjusted by defined microstructures, and thus the haptics. By means of these soft-touch structures, the friction values can also be defined in a direction-dependent manner. The frictional behavior of these micro-scale textures is determined by the properties of the stratum corneum. Considering the stratum corneum has a high elastic modulus, optimization of topography produced by laser texturing is expected that surfaces have very low friction [4]. For example, a pillar diameter of 45 µm with a depth of 10 µm has been micro processed in a stainless-steel plate, as shown in Figure 32. The structure was replicated with Silicone and is shown in Figure 33.

The coefficient of friction decreases strongly with normal load compared to non structured areas. Especially at lower normal loads the friction is times lower and enables the so called “soft touch”.

7.2 Optical structures

Structuring of embossing dies with geometries of some 10 µm for the functionalization of surfaces for refractive-optical laser mass production tools will be covered by typical refractive-optical structures like micro lenses. These topographies can then be transferred to a film which

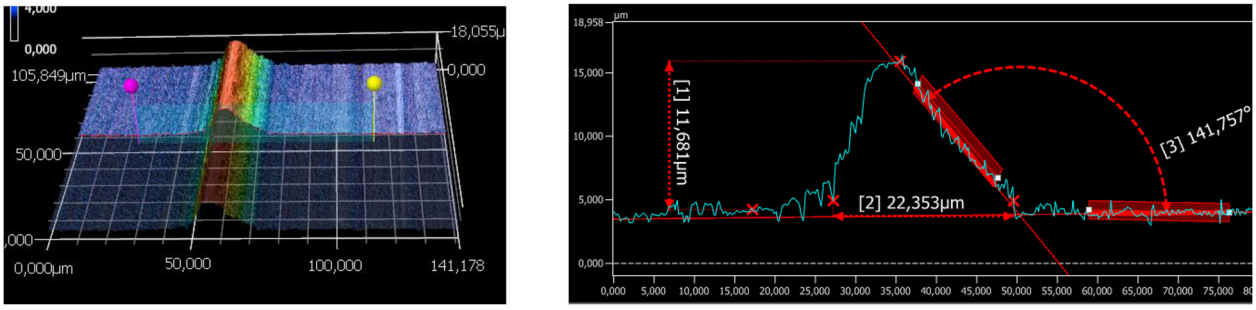

Figure 34: Refractive 3D micro Fresnel element, Cu *left*: 3D element, *right*: Cross section view..

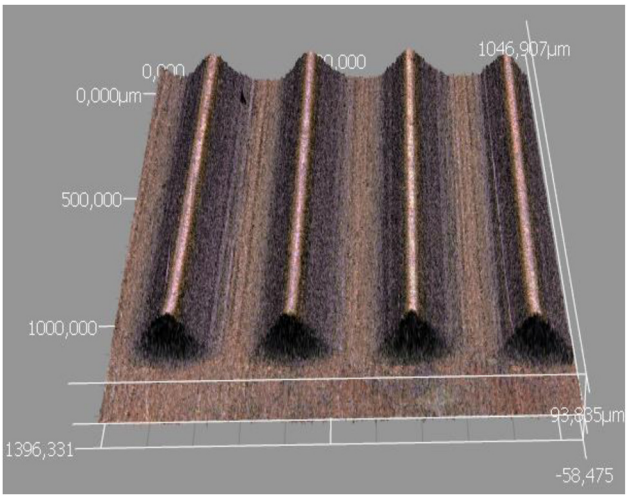

Figure 35: Micro prism array, distance: 250 µm, depth: 50 µm, Cu.

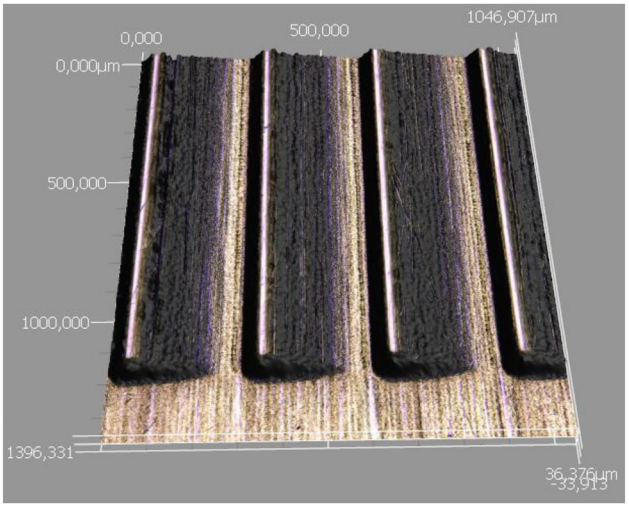

Figure 36: Fresnel lens, distance: 250 µm, depth:50 µm, Cu.

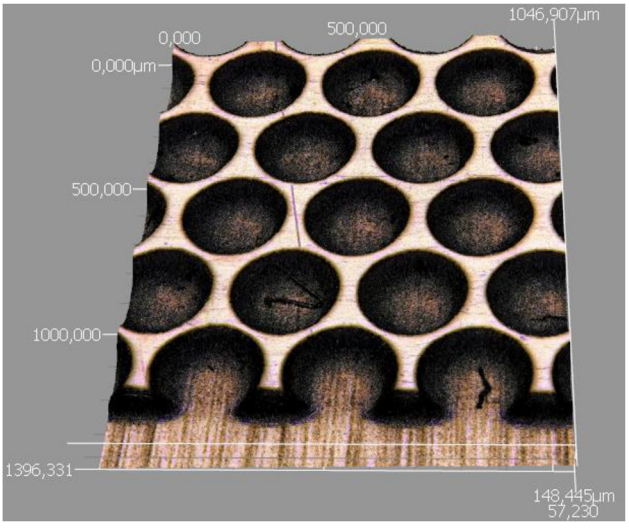

Figure 37: Concave lens array, diameter: 170 µm, depth 50 µm, Cu.

can be used for targeted light guidance in flat screens. Furthermore, the creation of surface structures by laser texturing with ultra short pulsed laser pulses has proven to be a useful technique for producing well-defined micro scale surface textures like diffractive structures.

7.2.1 Refractive µm-structure

For a light management application, optics in µm scale could be used for many products. Micro prisms with a base length of 22 µm were directly processed. In a first step, a continuous 3D structure was digitally generated in a pixel based 8-bit data asset (pixel size 500 nm). The data was transferred, pixel by pixel, onto a copper surface, as shown in Figure 34. The prism was engraved with a depth of approx. 10 µm in 20 passes (depth per pass 500 nm). The laser processed positive structure could be inverted into a negative structure on the final foil in an embossing/printing process.

Further technical 3D microstructures were investigated on copper surfaces. A variety of 3D structures enables functionalities for hot stamping applications in different kind of plastics, e.g. optical elements like prisms, Fresnel lenses, and lenses (Figures 35–38). Manufactured analogous to the structure shown in Figure 34.

With individual pulse-burst settings the ablation quality (burr, residue, and surface roughness) is adjustable. A positive side effect is the increased ablation rate which reduces the processing time significantly.

7.2.2 Diffractive structure

Diffractive optical structures are used as security elements in the packaging industry to avoid product piracy. As food

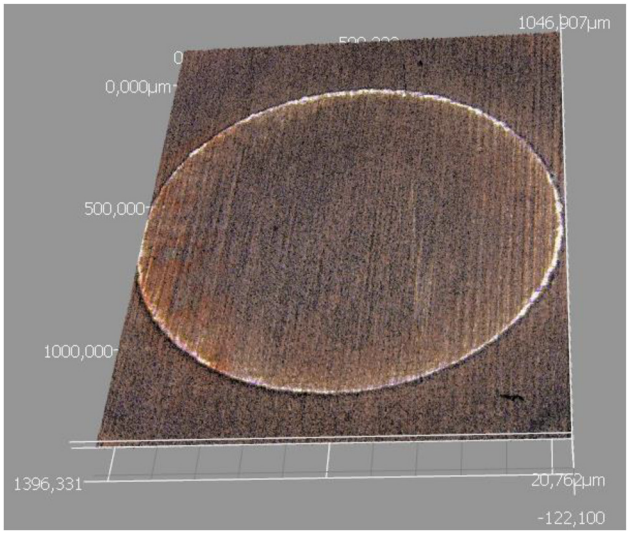

Figure 38: Parabolic surface, diameter: 1000 µm, depth 50 µm, Cu.

is mostly packed up in single use packages, these security elements must be manufactured in a low-cost roll-to-roll mass production. This means that diffractive structures must be laser processed on a cylinder that could be used as a mass production tool. In Figure 39, a detail view of a micro structured diffractive element with a resolution of 4 µm is shown. The depth was adjusted by the grey value of the pixel and was processed during the micro structuring process by controlling the laser fluence. A cylinder tool with this structure could be reproduced on foils in a rotary UV-Nano Imprint process [1].

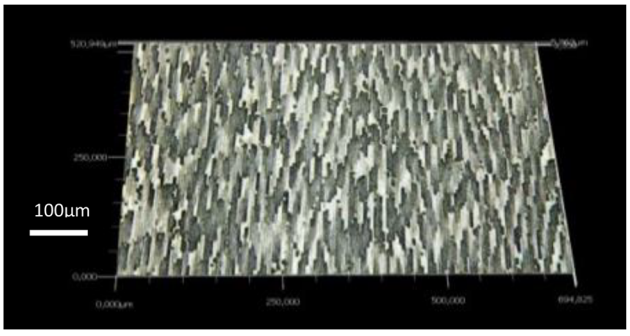

Figure 39: In stainless steel engraved diffractive structure, pixel size: 4 µm, depth 1.4 µm, 30 steps.

7.3 R2R mass production of Biological structures

7.3.1 Micro processing bio medical structures

Surface topographies designed by features with heights of 5 µm, arranged in an imaginary square with sizes of 10 by 10, 20 by 20, or 28 by 28 µm^2, lead to a significant cell growth. These features are built up by using microscale primitive geometries like circles, isosceles triangles, and thin rectangles. For the adjustment of the functionalities, computer based mathematical algorithms are used. The variety of cells and bacteria is high, and thus also the behavior of the organisms is different. This means that the micro structure must be adjusted to the habits of living cells. Therefore, several thousands of distinct, randomly designed surface topographies are necessary to enable the desired functionality [6]. For example, primitive shapes of

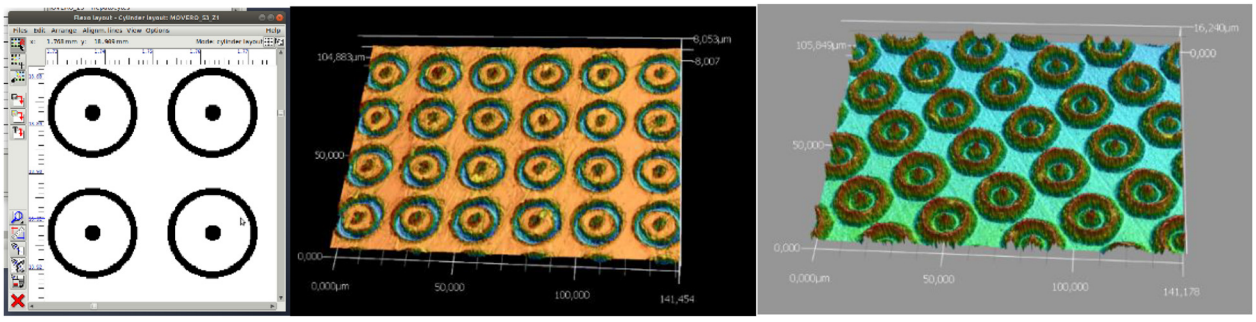

Figure 40: **Left**: Data asset bio medical structure, **middle**: Laser engraved in copper, **right**: Embossed sample.

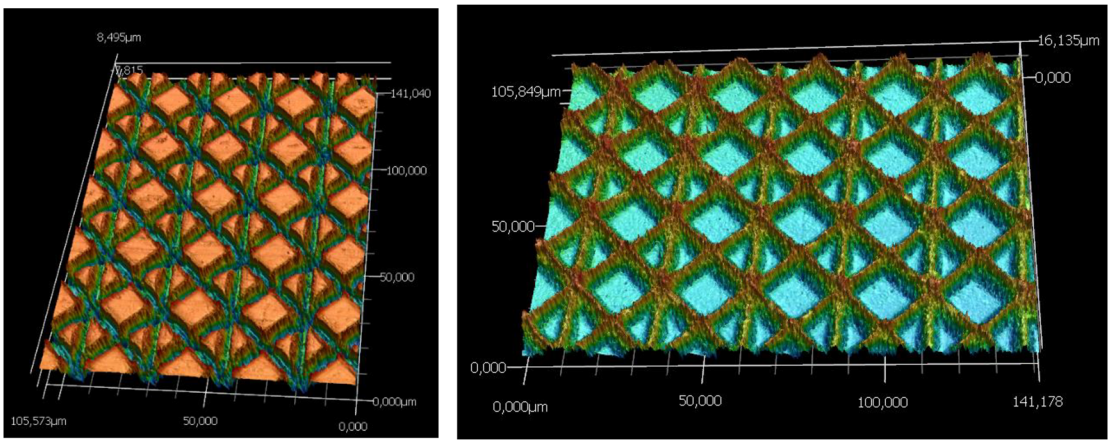

Figure 41: **Left**: Laser engraved hydrophobic structure in copper, **right**: Embossed sample.

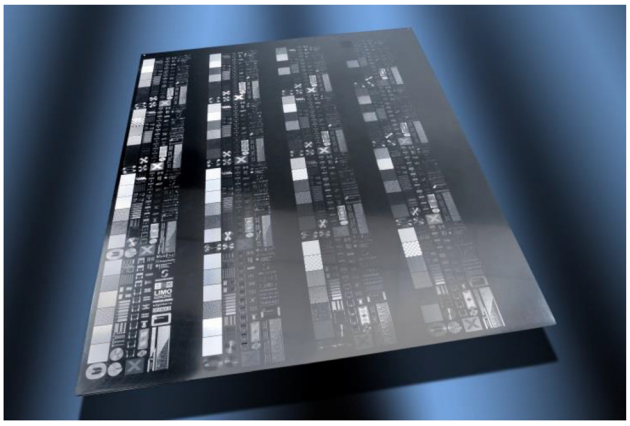

Figure 42: Embossing plate, 1 m × 1.2 m, microstructured with 8 spots, Cu with chrome coating.

pins with a diameter of 4 µm and circles with a diameter of 18 µm (Figure 40, Left) are processed in one step by a ultrashort pulsed laser engraving process on a copper surface (Figure 40, Middle), and reproduced in Silicone (Figure 40, Right)

7.3.2 Micro processing antibacterial structures

Today antibacterial properties are usually achieved by chemical modifications of surfaces. These chemical processes are not always safe and therefore not approved for all applications. In this contribution, antibacterial surfaces are processed whose function is based only on the structuring of the surface. This eliminates questionable additives and this result can be transferred to a variety of other applications. The typical dimensions of antibacterial structures are in the range of 1–5 µm. This pixel-based structure was engraved into a copper surface (Figure 41, Left).

The negative structure of the laser processed plate was embossed onto a plastic substrate (Figure 41, Right). In this manner a regular triplet structure was achieved. This example demonstrates the freedom of this processing method compared to laser induced periodic surface structures (LIPSS) or laser interference patterning. At least a computer simulated antibacterial structure could be used in a mass production application.

8 Conclusion

In this paper, an 8, respectively, 16 spot approach for UKP-laser processing with high quality and high throughput have been described achieving quite high ablation rates. The ablation rate achieved with a 300 W laser modulated into 8 beams with a spot diameter of 10 µm is 16.3 mm^3/min. In a further step this concept has been extended to 16 beamlets. With a processing resolution of 5080 dpi, the ablation rate could be increased to 27 mm^3/min.

By means of these process technologies, tools for the roll-to-roll fabrication for the embossing of optical, haptic, antiseptic, cell-growth-promoting, and optical-diffractive structures have been produced. The properties of surfaces can be significantly influenced by applying specific functional microstructures. The size of these structures varies depending on the function. The size and complexity, in turn, define the necessary resolution and the process technology. To realize the features in the µm-range on large areas (e.g. 1 × 1.2 m, Figure 42) in µm precision is still a challenge. But the way is paved to produce embossing shims in a single-stage production process without the use of wet-chemical process steps.

Author contributions: All the authors have accepted responsibility for the entire content of this submitted manuscript and approved submission.
Research funding: None declared.
Conflict of interest statement: The authors declare no conflicts of interest regarding this article.

References

[1] T. Bastuck, "Skalierbarkeit von Rolle-zu-Rolle-UV-Nanoimprint-Prozessen", PhD Thesis, Ergebnisse aus der Produktionstechnik, RWTH Aachen, 2020.
[2] C. Momma, S. Nolte, B. N. v Chivkov, F. Alvensleben, and A. Tünnermann, "Precise laser ablation with ultrashort pulses," *Appl. Surf. Sci.*, vols 109/110, pp. 15–19, 1997.
[3] E. G. Gamaly, A. V. Rode, and V. T. Tikhonchuk, "Luther-Davies, "Ablation of solids by femtosecond lasers: ablation mechanism and ablation threshold for metals and dielectrics"," *Phys. Rev.*, vol. A23, pp. 949–957, 2001.
[4] S. Bruening, G. Hennig, S. Eifel, and A. Gillner, "Ultra-fast scan techniques for 3D-micro structuring of metal surfaces with high repetitive ps-laser pulses" in "Ultra-fast scan technikques for 3D-micro structuring of metal surfaces with high repetitive ps-laser pulses," in *LiM, Laser in manufacturing*, Munich, 2011.
[5] Daijun Li and Keming Du, "Picosecond laser with 400 W average power and 1 mJ pulse energy," *Proc. SPIE*, vol. 7912, p. 79100N, 2011.
[6] K. Du, S. Bruening, and A. Gillner, *Compact High Power Ps-Laser and its Application in Large Area Engraving*, San Francisco, Photonics West, 2012.
[7] S. Bruening, PIKOFLAT-"System- und Verfahrenstechnik zur Großflächenstrukturierung mit Hochleistungs-Pikosekundenlasern", BMBF Project Report, 2012.
[8] S. Bruening, K. Du, M. Jarczynski, and A. Gillner, "High-throughput micro machining with ultrashort pulsed lasers and multiple spots," *J. Laser Appl.*, vol. 32, 2020, Art no. 012003.

[9] S. Bruening, K. Du, and A. Gillner, "Ultra-fast micromachining with multiple ultra-short pulsed laser sources," *Physics Procedia*, vol. 83, pp. 167–181, 2016.
[10] MultiSurf, Mikro- und nanoskalige Oberflächenfunktionalisierung durch Multistrahl-Laserverfahren", BMBF Project, 2018. Available at: http://www.photonikforschung.de/fileaadmin/Verbundsteckbriefe/19._Funktionale_Oberflaechen_und_Schichten/Multisurf-Projektsteckbrief-Oberflaechen-bf.pdf.
[11] S. Bruening, M. Jarczynski, T. Mitra, K. Du, C. Fornaroli, and A. Gillner, "Ultra-fast multi-spot-parallel processing of functional micro- and nano scale structures on embossing dies with ultrafast lasers", in *Proceedings of Lasers in Manufacturing LiM*, 2017.